

Rethinking the Power of Timestamps for Robust Time Series Forecasting: A Global-Local Fusion Perspective

Chengsen Wang^{1*} Qi Qi^{1*} Jingyu Wang^{12†}
 Haifeng Sun¹ Zirui Zhuang¹ Jinming Wu¹ Jianxin Liao¹

¹Beijing University of Posts and Telecommunications, Beijing, China

²Pengcheng Laboratory, Shenzhen, China

{cswang, qiqi8266, wangjingyu}@bupt.edu.cn
 {hf sun, zhuangzirui, wjm_18, liao jx}@bupt.edu.cn

Abstract

Time series forecasting has played a pivotal role across various industries, including finance, transportation, energy, healthcare, and climate. Due to the abundant seasonal information they contain, timestamps possess the potential to offer robust global guidance for forecasting techniques. However, existing works primarily focus on local observations, with timestamps being treated merely as an optional supplement that remains underutilized. When data gathered from the real world is polluted, the absence of global information will damage the robust prediction capability of these algorithms. To address these problems, we propose a novel framework named GLAFF. Within this framework, the timestamps are modeled individually to capture the global dependencies. Working as a plugin, GLAFF adaptively adjusts the combined weights for global and local information, enabling seamless collaboration with any time series forecasting backbone. Extensive experiments conducted on nine real-world datasets demonstrate that GLAFF significantly enhances the average performance of widely used mainstream forecasting models by 12.5%, surpassing the previous state-of-the-art method by 5.5%. Code is available at <https://github.com/ForestsKing/GLAFF>.

1 Introduction

Time series forecasting holds significant importance across various industries, including finance [1, 12], transportation [4, 11], energy [28, 31], healthcare [16, 29], and climate [8, 44]. With the development of deep learning techniques, neural network-based methods [15, 18, 40, 47] have notably propelled advancements owing to their strong capability in capturing dependencies within time series. The relevant models have evolved from statistical models to RNNs, CNNs, Transformers, and LLMs. However, existing research primarily concentrates on local observations within history sliding windows, overlooking the significance of timestamps.

Due to the abundant seasonal information they contain, timestamps possess the potential to offer robust global guidance for forecasting techniques. For instance, traffic volumes on weekdays typically exhibit high peaks. Regrettably, existing works primarily focus on local observations, with timestamps being treated merely as an optional supplement that remains underutilized. DLinear [41] and FPT [47] completely overlook timestamps. Informer [45] and TimesNet [38] incorporate timestamps by summing their embeddings with position embeddings and data embeddings. These intertwined

*Equal contribution.

†Corresponding author.

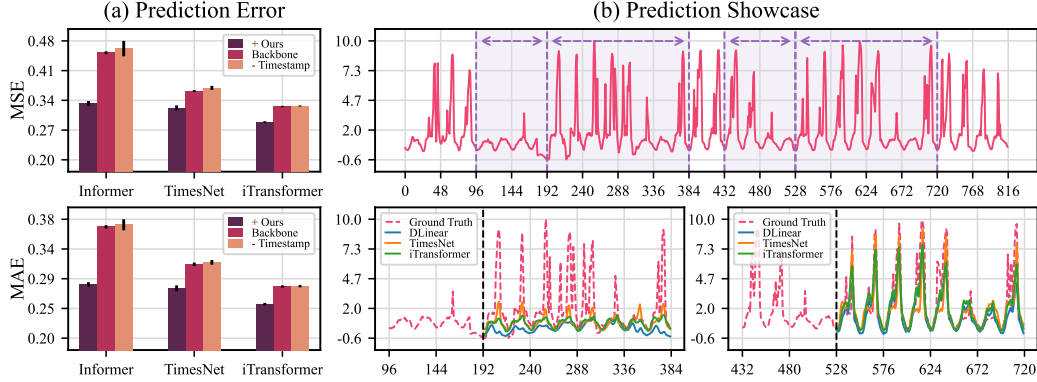


Figure 1: The experimental results on Traffic dataset. (a) illustrates the outcomes of the ablation study on mainstream forecasting models and their variants. (b) depicts the visualization of traffic volume (upper), successful prediction case (lower right), and failed prediction case (lower left), respectively.

patterns encourage networks to extract information from more intuitive observations. iTransformer [24] embeds timestamp features separately into tokens employed by the attention mechanism. This embedding method across time points damaged the physical significance of timestamps. To validate this proposition, we conduct an ablation study on the aforementioned models using the Traffic dataset. The results depicted in Figure 1(a) indicate that the performance of the models exhibits no significant decline after removing timestamps. Meanwhile, our proposed GLAFF demonstrates a notable enhancement in mainstream forecasting models.

Moreover, Time series collected from the real world often be polluted [5]. For example, a spike in electricity consumption coupled with short circuits can induce point anomalies, while a reduction in traffic volume coinciding with holidays can evoke contextual anomalies. When local information gathered from the real world contains anomalies, the absence of global information will damage the robust prediction capability of most forecasting techniques [7, 39, 43, 46]. We illustrate traffic volume for San Francisco Bay area freeways at an hourly granularity in Figure 1(b). Typically, this sequence exhibits a clear periodic pattern, alternating with five high peaks (weekdays) and two low peaks (weekends). However, due to a holiday, the week from 24 to 192 shows a deviation, resulting in three high peaks and four low peaks. As evident from the illustration in the lower right corner of Figure 1(b), the mainstream forecasting models [24, 38, 41] usually demonstrate reliable prediction capability. Nonetheless, when the observations within the history window include anomalies, as illustrated in the lower left corner of Figure 1(b), these models are significantly affected and yield notably underestimated predictions. Therefore, it is necessary to reasonably incorporate more robust global information into the existing forecasting technique.

To address the aforementioned problems, we propose a generalized framework named GLAFF (short for **G**lobal-**L**ocal **A**daptive **F**usion **F**ramework), aimed at enhancing the robust prediction capability of time series forecasting models in the real world leveraging global information. Specifically, GLAFF initially employs the Attention-based Mapper to individually model the timestamps containing global information and maps them to observations conforming to a standard distribution. Subsequently, to handle scenarios where anomalies are present within the observations of the sliding window, we utilize the Robust Denormalizer to inverse normalize the initial mappings, thereby mitigating the impact of data drift [17]. Finally, the Adaptive Combiner dynamically adjusts the combined weights for global mapping and local prediction within the prediction window, yielding the final prediction outcome. By fusing the robustness of global information with the flexibility of local information, GLAFF demonstrates a substantial enhancement in the robust prediction capability of mainstream forecasting models. Additionally, GLAFF serves as a model-agnostic and plug-and-play framework that can seamlessly collaborate with any time series forecasting backbone.

In general, the contributions of our paper are summarised as follows:

- We propose GLAFF that leverages global information, represented by timestamps, to improve the robust prediction capability of time series forecasting models. GLAFF is a plug-and-play module that seamlessly collaborates with any time series forecasting backbone.

- We design a Robust Denormalization module to facilitate the adaptation of GLAFF for data drift, even when the observations encompass anomalies, alongside an Adaptive Combiner module for dynamically fusing global and local information.
- We conduct comprehensive experiments on nine real-world benchmark datasets across five domains. The result demonstrates that GLAFF significantly improves the robust prediction capability of mainstream forecasting models.

2 Related Work

As a significant real-world challenge, time series forecasting has garnered considerable attention. Initially, ARIMA [2] establishes an autoregressive model and performs forecasts in a moving average manner. However, the inherent complexity of the real world often renders such statistical methodologies [2, 14, 33] challenging to adapt. With the development of deep learning techniques, neural network-based methods have become increasingly important. Recurrent neural networks [10, 13, 30] dynamically capture temporal dependencies by modeling semantic information within a sequential structure. Unfortunately, this architecture suffers from gradient vanishing/exploding and information forgetting when dealing with long sequences. To further improve prediction performance, self-attention mechanisms [19, 22, 45] and convolutional networks [21, 36, 38] have been introduced to capture long-range dependencies. Additionally, prior research [41] has demonstrated that a simple linear network augmented by decomposition can also achieve competitive performance. Nowadays, with fast growth and remarkable performances of large language models, there is a growing interest [3, 32, 47] in utilizing LLM to analyze time series data. Recently, the iTransformer [24] has emerged as the state-of-the-art method for time series forecasting tasks by embedding series from different channels into the variate tokens utilized by the attention mechanism.

Most time series forecasting techniques focus on local observations, with timestamps being treated merely as an optional supplement that remains underutilized. DLinear [41], FPT [47], and other models [26, 40, 43] completely overlook timestamps. When data gathered from the real world is polluted, the absence of global information will damage the robust prediction capability of these algorithms. Informer [45], TimesNet [38], and other models [23, 37, 46] incorporate timestamps by summing their embeddings with position embeddings and data embeddings. These intertwined patterns encourage networks to extract information from more intuitive observations. iTransformer [24] embeds timestamp features separately into tokens employed by the attention mechanism. This embedding method across time points damaged the physical significance of timestamps.

The processing of timestamps by the previous baselines and our proposed GLAFF can be abstracted as early fusion (feature-level fusion) and late fusion (decision-level fusion). Early fusion integrates modalities into a single representation at the input level and processes the fused representation through the model. Late fusion allows each modality to run independently through its own model and fuses the outputs of each modality. Compared to early fusion, late fusion maximizes the processing effectiveness of each modality and is less susceptible to the noise of a single modality, resulting in greater robustness and reliability. This has been validated by extensive previous work [20, 27, 35].

3 Methodology

We propose a model-agnostic and plug-and-play framework, GLAFF, which utilizes global information, represented by timestamps, to enhance the robust prediction capability of mainstream time series forecasting models in real-world scenarios. In multivariate time series forecasting, given the history observations of c channels within h time steps $\mathbf{X} = \{\mathbf{x}_1, \dots, \mathbf{x}_h\} \in \mathbb{R}^{h \times c}$, we aim to forecast the subsequent p time steps $\mathbf{Y} = \{\mathbf{x}_{h+1}, \dots, \mathbf{x}_{h+p}\} \in \mathbb{R}^{p \times c}$. In addition to observations, we incorporate timestamps to provide global information. For each timestamp, we extract its month, day, weekday, hour, minute, and second as timestamp features, respectively. For instance, for the timestamp *2018-06-02 12:00:00* at moment t , its feature representation is $\mathbf{s}_t = [06, 02, 05, 12, 00, 00] \in \mathbb{R}^{1 \times 6}$. The holiday markers may also be included if accessible. Unlike observations, the timestamp features within the history window $\mathbf{S} = \{\mathbf{s}_1, \dots, \mathbf{s}_h\} \in \mathbb{R}^{h \times 6}$ and the timestamp features within the prediction window $\mathbf{T} = \{\mathbf{s}_{h+1}, \dots, \mathbf{s}_{h+p}\} \in \mathbb{R}^{p \times 6}$ are known. In this section, we describe the detailed workflow of the entire GLAFF framework and explain how it fuses local information \mathbf{X} and global information \mathbf{S}, \mathbf{T} to predict \mathbf{Y} .

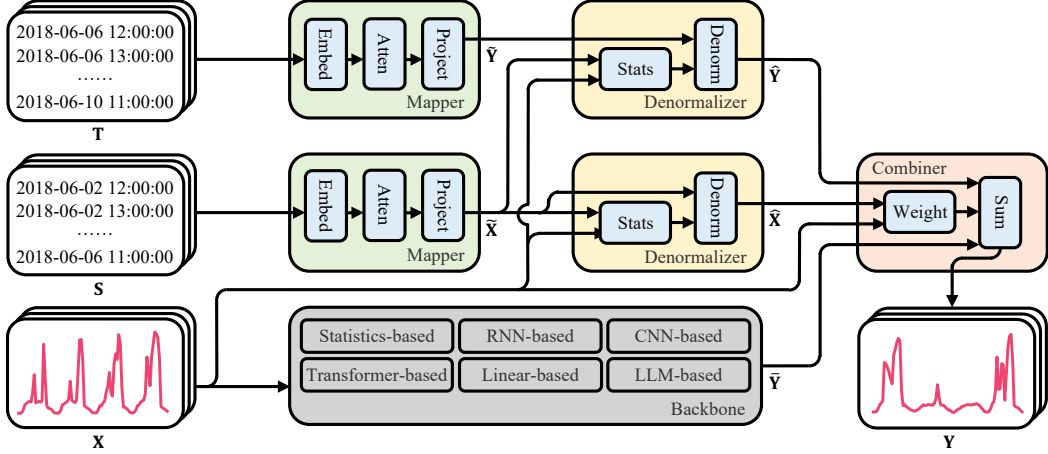


Figure 2: The overall architecture of GLAFF mainly consists of three primary components: Attention-based Mapper, Robust Denormalizer, and Adaptive Combiner.

3.1 Overview

GLAFF is a plug-and-play framework that seamlessly collaborates with any time series forecasting backbone. The overall architecture of the plugin is depicted in Figure 2, comprising three primary components: Attention-based Mapper, Robust Denormalizer, and Adaptive Combiner. Following local prediction $\hat{Y} \in \mathbb{R}^{p \times c}$ provided by the backbone network based on history observations \mathbf{X} (maybe including underutilized history timestamps \mathbf{S} and future timestamps \mathbf{T}), GLAFF leverages global information to revise it. Initially, the Attention-based Mapper captures dependencies between timestamps through an attention mechanism, mapping timestamp features \mathbf{S} and \mathbf{T} into an initial history mapping $\tilde{\mathbf{X}} \in \mathbb{R}^{h \times c}$ and an initial future mapping $\tilde{\mathbf{Y}} \in \mathbb{R}^{p \times c}$, conforming to standard distribution. Subsequently, the Robust Denormalizer inverse normalizes the initial mappings $\tilde{\mathbf{X}}$ and $\tilde{\mathbf{Y}}$ to $\hat{\mathbf{X}} \in \mathbb{R}^{h \times c}$ and $\hat{\mathbf{Y}} \in \mathbb{R}^{p \times c}$ based on quantile deviation between the initial mapping $\tilde{\mathbf{X}}$ and the actual observations \mathbf{X} within the history window, mitigating the impact of data drift. Lastly, the Adaptive Combiner dynamically adjusts the combined weights of the global mapping $\hat{\mathbf{Y}}$ and the local prediction $\hat{\mathbf{Y}}$ within the prediction window according to the disparity between the final mapping $\hat{\mathbf{X}}$ and the actual observations \mathbf{X} within the history window, yielding the final prediction outcome \mathbf{Y} . By fusing the robustness of global information and the flexibility of local information, GLAFF significantly enhances the robust prediction capability of mainstream forecasting models.

3.2 Attention-based Mapper

As depicted in the green segment of Figure 2, our proposed Attention-based Mapper employs a simplified encoder-only architecture within the Transformer [34] framework, comprising an embedding layer, attention blocks, and a projection layer. Analogous to typical Transformer-based encoders [37, 45], each timestamp feature is initially tokenized by an embedding layer to describe its properties, applied by self-attention for mutual interactions, and individually processed by feed-forward networks for series representations. Subsequently, a projection layer is utilized to acquire the initial mappings. Leveraging the capability of the attention mechanism for capturing long-range dependencies and parallel computation, the Attention-based Mapper can sufficiently model the global information embodied by timestamps.

Specifically, in Attention-based Mapper, the procedure for obtaining its corresponding initial mapping $\tilde{\mathbf{X}}$, which conforms to the standard distribution, based on the history timestamps \mathbf{S} , is succinctly delineated as follows:

$$\begin{aligned}
 \mathbf{H}^0 &= \text{Embedding}(\mathbf{S}) \\
 \mathbf{H}^{i+1} &= \text{Attention}(\mathbf{H}^i), \quad i = 0, \dots, l-1 \\
 \tilde{\mathbf{X}} &= \text{Projection}(\mathbf{H}^l)
 \end{aligned} \tag{1}$$

where $\mathbf{H}^i \in \mathbb{R}^{h \times d}$ denotes the intermediate feature variable output from the i -th attention block, and d represents the dimension of the intermediate feature variable. The attention blocks are stacked with l layers to capture the high-level semantic information hidden within the timestamps. To maintain simplicity in implementation, both the embedding and projection layers are comprised of a single linear layer. Following conventional protocol, the primary computation steps for the i -th attention block are outlined as:

$$\begin{aligned}\mathbf{H}^i &= \text{LayerNorm}(\mathbf{H}^i + \text{MSA}(\mathbf{H}^i, \mathbf{H}^i, \mathbf{H}^i)) \\ \mathbf{H}^{i+1} &= \text{LayerNorm}(\mathbf{H}^i + \text{FeedForward}(\mathbf{H}^i))\end{aligned}\quad (2)$$

where $\text{LayerNorm}(\cdot)$ represents the commonly adopted layer normalization and $\text{FeedForward}(\cdot)$ denotes the multilayer feedforward network. The $\text{MSA}(\mathbf{Q}, \mathbf{K}, \mathbf{V})$ indicates the Multihead Self-Attention mechanism [34], where $\mathbf{Q}, \mathbf{K}, \mathbf{V}$ serve as the query, key, and value respectively. Additionally, a dropout mechanism is incorporated to alleviate overfitting and enhance the generalization of the network. The process of obtaining the corresponding initial mapping $\tilde{\mathbf{Y}}$ based on the future timestamps \mathbf{T} , conforming to the standard distribution, mirrors the aforementioned procedure, simply substituting \mathbf{S} and $\tilde{\mathbf{X}}$ in Equation 1 with \mathbf{T} and $\tilde{\mathbf{Y}}$ respectively.

3.3 Robust Denormalizer

Due to the inherent variability of the real world, time series observations typically undergo rapid evolution over time, a phenomenon commonly referred to as data drift [17]. This phenomenon can result in discrepancies across different time spans and hinder the generalization ability of deep learning models. Recognizing the presence of data drift, GLAFF employs a two-phase untangling modeling strategy to address the global information represented by timestamps. In the first phase, the network in Attention-based Mapper produces initial mappings, denoted as $\tilde{\mathbf{X}}$ and $\tilde{\mathbf{Y}}$, which are assumed to satisfy a standard distribution for reducing the difficulty of modeling the dependencies between timestamps and observations. Subsequently, in the second phase, leveraging the distribution deviations between the initial mapping $\tilde{\mathbf{X}}$ and the actual observations \mathbf{X} within the history window, the Robust Denormalizer separately inverse normalizes the initial mappings $\tilde{\mathbf{X}}$ and $\tilde{\mathbf{Y}}$ to produce the final mappings $\hat{\mathbf{X}}$ and $\hat{\mathbf{Y}}$, mitigating the impact of data drift.

To alleviate the impact of data drift, a feasible solution [9, 17, 23, 25] has been proposed: removing dynamic factors from the original data through a normalization procedure before feeding them into the deep learning model, and subsequently reintroducing these dynamic factors via an inverse normalization procedure after output from the deep learning model. The conventional inverse normalization procedure typically considers distribution deviations in mean and standard deviation. Nonetheless, this approach is susceptible to extreme values and lacks robustness when the observations contain anomalies. Instead of relying on mean and standard deviation, we employ median and quantile ranges [6], respectively, to enhance the robustness of the Robust Denormalizer against anomalies. As depicted in the yellow segment of Figure 2, the procedure for Robust Denormalizer to inverse normalize initial mappings $\tilde{\mathbf{X}}$ and $\tilde{\mathbf{Y}}$ into final mappings $\hat{\mathbf{X}}$ and $\hat{\mathbf{Y}}$ can be succinctly expressed as:

$$\begin{aligned}\hat{\mathbf{X}} &= \tilde{\mathbf{X}} \times \left(\frac{\sigma}{\tilde{\sigma}} \right) + (\mu - \tilde{\mu}) \\ \hat{\mathbf{Y}} &= \tilde{\mathbf{Y}} \times \left(\frac{\sigma}{\tilde{\sigma}} \right) + (\mu - \tilde{\mu})\end{aligned}\quad (3)$$

where $\tilde{\mu} \in \mathbb{R}^{1 \times c}$ and $\mu \in \mathbb{R}^{1 \times c}$ represent the median of the initial mapping $\tilde{\mathbf{X}}$ and the actual observation \mathbf{X} for each channel, respectively. Similarly, $\tilde{\sigma} \in \mathbb{R}^{1 \times c}$ and $\sigma \in \mathbb{R}^{1 \times c}$ denote the quantile range (the distance between the q quantile and the $1 - q$ quantile) of the initial mapping $\tilde{\mathbf{X}}$ and the actual observation \mathbf{X} for each channel. Specifically, when $q = 0.75$, $\tilde{\sigma}$ and σ correspond to the inter-quartile range (IQR³) for each channel of the initial mapping $\tilde{\mathbf{X}}$ and the actual observation \mathbf{X} .

3.4 Adaptive Combiner

Owing to the intricacies of real-world scenarios, data preferences for model bias will continuously change with online concept drifts [42]. Therefore, we need a data-dependent strategy to change

³IQR is defined as the difference between the 1st and 3rd quartiles of a distribution or set of values, and is a robust measure of the distribution spread.

the model selection policy continuously. In other words, the combined weights of global and local information necessitate adaptive and dynamic updates. When the time series pattern exhibits clarity and stability, greater emphasis should be placed on robust global information. Conversely, increased attention should be directed towards flexible local information when the time series pattern appears ambiguous and variable. Within the framework of GLAFF, we employ an Adaptive Combiner to realize the adaptive adjustment of combined weights.

As illustrated in the red segment of Figure 2, the Adaptive Combiner initially dynamically adjusts the combined weights of the global mapping $\hat{\mathbf{Y}}$ and the local prediction $\bar{\mathbf{Y}}$ within the prediction window, based on the deviation between the final mapping $\hat{\mathbf{X}}$ and the actual observation \mathbf{X} within the history window. Subsequently, we aggregate the dual-source information based on the combined weights to yield the final prediction \mathbf{Y} . Specifically, the primary computation procedure of the Adaptive Combiner is represented as:

$$\begin{aligned}\mathbf{W} &= \text{MLP}(\hat{\mathbf{X}} - \mathbf{X}) \\ \mathbf{Y} &= \sum \mathbf{W} \times (\hat{\mathbf{Y}} \oplus \bar{\mathbf{Y}})\end{aligned}\tag{4}$$

where $\mathbf{W} \in \mathbb{R}^{1 \times c \times 2}$ signifies the dynamically generated combined weight by the network based on the deviation between the final mapping $\hat{\mathbf{X}}$ and the actual observation \mathbf{X} within the history window. The \oplus denotes the concatenation operation based on the additional last dimension, and \sum denotes the summation operation performed across the last dimension. For simplicity, the weight generation network consists solely of a Multilayer Perceptron (MLP) containing a hidden layer and a layer of Softmax for weight normalization.

Through adaptive adjustment of combined weights, our method can effectively fuses the robustness of global information and the flexibility of local information, thereby enhancing its suitability for intricate and fluctuating real-world scenarios.

4 Experiment

4.1 Experimental Setup

Dataset We conduct extensive experiments on nine datasets across five domains, including Electricity, Exchange, Traffic, Weather, and ILI, along with four ETT datasets. Detailed dataset information is provided in Appendix A.1. We follow the standard segmentation protocol [24, 37, 45], strictly dividing each dataset into training, validation, and testing sets chronologically to ensure no information leakage issues. The segmentation ratio for each dataset is set to 6:2:2. Regarding prediction settings, we also adhere to established mainstream protocols [26, 38, 41]. Specifically, we set the length of the history window to 96 for the Electricity, Exchange, Traffic, Weather, and four ETT datasets, while the prediction length varies within {96, 192, 336, 720}. For the ILI, which has fewer time points, the length of the history window is fixed at 36, and the prediction length varies within {24, 36, 48, 60}.

Backbone To demonstrate the effectiveness of the framework, we select several mainstream forecasting models based on different architectures, including the Transformer-based Informer (2021) [45] and iTransformer (2024) [24], the Linear-based DLinear (2023) [41], and the Convolution-based TimesNet (2023) [38]. Notably, iTransformer represents the previous state-of-the-art method in time series forecasting tasks. Further details regarding the backbone models are provided in Appendix A.2. As described in Section 2, these backbones encompass three different treatments for timestamps employed in prior forecasting techniques, namely summation (Informer, TimesNet), concatenation (iTransformer), and omission (DLinear).

The details of experimental setup can be found in Appendix A.3. All experiments are based on our runs, utilizing the same hardware configurations, and repeated 3 times with different random seeds.

4.2 Main Result

Table 1 compares the prediction outcomes for mainstream baselines and GLAFF. We present a detailed version of this table in Appendix B.1. The results indicate that GLAFF significantly surpasses all four widely used mainstream baselines across all nine real-world benchmark datasets. In particular, GLAFF enhances the respective backbones by an average of 12.5%.

Table 1: The forecasting errors for multivariate time series among GLAFF and mainstream baselines. A lower outcome indicates a better prediction. The best results are highlighted in bold.

Method	Informer				+ Ours				DLinear				+ Ours				TimesNet				+ Ours				iTransformer				+ Ours				Impr.
	MSE	MAE	MSE	MAE	MSE	MAE	MSE	MAE	MSE	MAE	MSE	MAE	MSE	MAE	MSE	MAE	MSE	MAE	MSE	MAE	MSE	MAE	MSE	MAE	MSE	MAE	MSE	MAE					
Electricity	96	0.333	0.414	0.217	0.323	0.196	0.283	0.147	0.238	0.175	0.280	0.154	0.248	0.153	0.246	0.120	0.198	15.7%															
	192	0.362	0.444	0.220	0.329	0.196	0.286	0.172	0.253	0.191	0.293	0.169	0.261	0.167	0.259	0.143	0.216																
	336	0.352	0.434	0.230	0.337	0.208	0.301	0.197	0.274	0.211	0.310	0.185	0.276	0.183	0.276	0.168	0.240																
	720	0.364	0.443	0.247	0.351	0.239	0.331	0.239	0.308	0.235	0.326	0.226	0.303	0.220	0.310	0.217	0.279																
ETTh1	96	0.926	0.736	0.609	0.569	0.409	0.440	0.391	0.418	0.453	0.481	0.435	0.464	0.420	0.454	0.411	0.441	8.8%															
	192	1.235	0.844	0.831	0.680	0.457	0.475	0.446	0.457	0.533	0.531	0.520	0.517	0.494	0.502	0.474	0.482																
	336	1.354	0.875	0.882	0.698	0.500	0.506	0.492	0.488	0.621	0.580	0.596	0.560	0.538	0.528	0.534	0.519																
	720	1.264	0.857	0.937	0.730	0.610	0.576	0.609	0.556	0.844	0.697	0.773	0.661	0.716	0.629	0.704	0.615																
ETTh2	96	0.708	0.549	0.422	0.443	0.159	0.278	0.128	0.205	0.183	0.298	0.174	0.276	0.177	0.287	0.172	0.271	12.1%															
	192	1.133	0.688	0.860	0.599	0.187	0.309	0.165	0.238	0.218	0.329	0.204	0.306	0.199	0.311	0.196	0.295																
	336	0.997	0.667	0.747	0.570	0.207	0.330	0.206	0.265	0.240	0.346	0.219	0.319	0.220	0.329	0.213	0.306																
	720	1.607	0.815	1.255	0.720	0.262	0.378	0.214	0.288	0.281	0.376	0.278	0.363	0.271	0.366	0.270	0.356																
ETTm1	96	0.593	0.548	0.503	0.486	0.339	0.388	0.309	0.353	0.449	0.448	0.381	0.398	0.383	0.415	0.349	0.386	8.1%															
	192	0.611	0.576	0.534	0.525	0.394	0.418	0.362	0.386	0.448	0.461	0.440	0.432	0.429	0.445	0.403	0.420																
	336	0.888	0.726	0.707	0.628	0.450	0.451	0.442	0.432	0.550	0.504	0.494	0.462	0.485	0.479	0.468	0.460																
	720	1.037	0.786	0.925	0.719	0.508	0.493	0.493	0.467	0.619	0.559	0.563	0.507	0.566	0.532	0.564	0.519																
ETTm2	96	0.186	0.311	0.147	0.266	0.115	0.232	0.080	0.165	0.121	0.234	0.110	0.212	0.120	0.235	0.111	0.221	12.1%															
	192	0.242	0.348	0.230	0.341	0.143	0.261	0.109	0.193	0.155	0.267	0.136	0.239	0.149	0.266	0.144	0.252																
	336	0.454	0.466	0.308	0.380	0.176	0.294	0.148	0.229	0.190	0.293	0.175	0.269	0.185	0.293	0.182	0.283																
	720	0.861	0.616	0.719	0.561	0.225	0.340	0.221	0.274	0.242	0.334	0.225	0.309	0.233	0.333	0.232	0.327																
Exchange	96	0.735	0.728	0.223	0.391	0.051	0.164	0.046	0.155	0.076	0.198	0.066	0.177	0.058	0.172	0.051	0.158	16.4%															
	192	1.016	0.861	0.421	0.547	0.099	0.238	0.093	0.225	0.135	0.272	0.115	0.242	0.113	0.245	0.108	0.231																
	336	1.331	0.971	0.691	0.694	0.174	0.317	0.161	0.299	0.237	0.363	0.219	0.336	0.210	0.339	0.196	0.314																
	720	2.054	1.263	1.152	0.922	0.314	0.446	0.308	0.439	0.636	0.618	0.595	0.582	0.517	0.551	0.510	0.529																
ILI	24	3.374	1.356	2.487	1.106	2.087	1.131	1.875	0.963	1.478	0.713	1.333	0.684	1.148	0.659	1.129	0.658	9.9%															
	36	3.094	1.293	2.617	1.157	2.065	1.107	1.756	0.957	1.294	0.748	1.204	0.695	1.061	0.695	1.039	0.682																
	48	3.383	1.370	2.879	1.230	2.059	1.088	1.639	0.912	1.280	0.736	1.278	0.721	1.209	0.735	1.164	0.715																
	60	3.610	1.415	3.086	1.274	2.186	1.097	1.644	0.889	1.291	0.773	1.191	0.713	1.222	0.758	1.196	0.731	1.222	0.758	1.196	0.731	1.222	0.758	1.196	<b								

Table 2: The forecasting errors for multivariate time series among GLAFF and LLM-based baselines. A lower outcome indicates a better prediction. The best results are highlighted in bold.

Method	GPT2(3)				GPT2(6)			
	MSE	MAE	MSE	MAE	MSE	MAE	MSE	MAE
Electricity	0.194±0.002	0.278±0.002	0.168±0.005	0.258±0.002	0.194±0.001	0.279±0.002	0.171±0.002	0.258±0.001
ETTh1	0.466±0.001	0.483±0.001	0.454±0.003	0.462±0.003	0.468±0.002	0.483±0.002	0.445±0.002	0.451±0.002
ETTh2	0.190±0.000	0.304±0.000	0.178±0.017	0.284±0.010	0.190±0.002	0.303±0.002	0.177±0.005	0.286±0.003
ETTm1	0.411±0.005	0.431±0.003	0.388±0.009	0.409±0.005	0.412±0.002	0.431±0.002	0.390±0.012	0.413±0.007
ETTm2	0.142±0.001	0.257±0.001	0.120±0.001	0.235±0.002	0.142±0.002	0.256±0.002	0.119±0.002	0.233±0.002
Exchange	0.110±0.001	0.238±0.002	0.090±0.002	0.219±0.002	0.106±0.001	0.234±0.001	0.088±0.001	0.216±0.001
IL1	1.585±0.041	0.900±0.019	1.393±0.024	0.782±0.023	1.494±0.012	0.854±0.010	1.396±0.026	0.778±0.018
Traffic	0.370±0.002	0.309±0.002	0.296±0.002	0.256±0.001	0.371±0.002	0.312±0.001	0.301±0.003	0.262±0.002
Weather	0.241±0.000	0.276±0.000	0.234±0.004	0.268±0.003	0.243±0.001	0.278±0.001	0.228±0.002	0.264±0.002

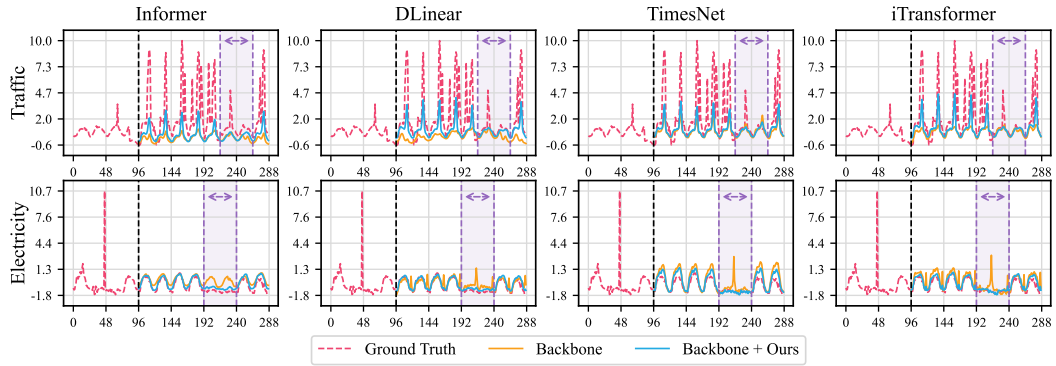


Figure 3: The illustration of prediction showcases among GLAFF and mainstream baselines.

Additionally, to validate the practical applicability of GLAFF, we assess the computation costs in Appendix B.4. The results indicate that GLAFF has little effect on model training and deployment across most scenarios, particularly when considering its significant accuracy enhancement.

4.3 Prediction Showcase

In addition to evaluation metrics, forecasting quality is crucial. To further compare GLAFF and the four mainstream forecasting models, we illustrate prediction showcases for two representative datasets in Figure 3. We provide the full prediction showcases for the nine datasets in Appendix B.5. It is evident that GLAFF can yield more realistically robust predictions. At the same time, the respective backbones are susceptible to abnormal local information.

The Traffic dataset records traffic volume in hourly granularity. Typically, this sequence exhibits a clear periodic pattern, alternating with five high peaks (weekdays) and two low peaks (weekends). However, owing to a holiday, the initial two days within the example history window do not exhibit the high peaks as usual. Due to the limited local information containing such contextual anomalies, Informer, DLinear, and iTransformer all think the prediction window should also consist of only low peaks. Although TimesNet generates predictions with high peaks, it displays an incorrect alternation between five high peaks and one low peak. By introducing sufficiently modeled global information, GLAFF has enabled the four mainstream forecasting backbones to recognize the existence of high peaks and the correct periodic patterns, thus yielding more accurate forecasts.

The Electricity dataset records electricity consumption in hourly granularity. Typically, this sequence exhibits a clear periodic pattern, alternating with five peaks (weekdays) and two flat segments (weekends). However, owing to a short circuit, the middle two days within the example history window show a spike in electricity consumption. Due to the limited local information containing such point anomalies, DLinear, TimesNet, and iTransformer all think the flat segments in the prediction window should also contain a spike. Although Informer generates predictions without spikes, it completely ignores the presence of flat segments. By introducing sufficiently modeled global information, GLAFF has enabled the four mainstream forecasting backbones to recognize the contingency of spikes and the correct periodic patterns, thus yielding more robust predictions.

Table 3: The forecasting errors for multivariate time series of ablation study among GLAFF and variants. A lower outcome indicates a better prediction. The best results are highlighted in bold.

Method	iTransformer				+ Ours		w/o Backbone		w/o Attention		w/o Quantile		w/o Adaptive	
	MSE	MAE	MSE	MAE	MSE	MAE	MSE	MAE	MSE	MAE	MSE	MAE	MSE	MAE
Electricity	96	0.1525	0.2460	0.1197	0.1979	0.2058	0.2663	0.1518	0.2450	0.1467	0.2465	0.1574	0.2502	
	192	0.1674	0.2593	0.1434	0.2157	0.2097	0.2793	0.1684	0.2610	0.1677	0.2662	0.1740	0.2662	
	336	0.1830	0.2762	0.1683	0.2395	0.2454	0.3014	0.1832	0.2775	0.1993	0.2954	0.1953	0.2877	
	720	0.2199	0.3097	0.2169	0.2786	0.2984	0.3386	0.2182	0.3092	0.2593	0.3403	0.2330	0.3171	
Traffic	96	0.3084	0.2717	0.2828	0.2485	0.3348	0.2723	0.3172	0.2806	0.2909	0.2684	0.2930	0.2612	
	192	0.3267	0.2794	0.2909	0.2528	0.3387	0.2736	0.3357	0.2884	0.2948	0.2737	0.2970	0.2610	
	336	0.3381	0.2850	0.3005	0.2594	0.3460	0.2794	0.3482	0.2958	0.3023	0.2804	0.3082	0.2706	
	720	0.3574	0.3015	0.3201	0.2730	0.3558	0.2906	0.3684	0.3113	0.3249	0.2984	0.3212	0.2819	
Avg.		0.2602	0.2827	0.2367	0.2593	0.3000	0.3004	0.2646	0.2870	0.2555	0.2876	0.2591	0.2845	

4.4 Ablation Study

We provide a comprehensive ablation study to validate the necessity of the GLAFF components. We implement our approach and its four variants on the iTransformer backbone. The results of our experiments on three representative benchmark datasets are presented in Table 3. Detailed results for the nine real-world benchmark datasets are available in Appendix B.2.

In w/o Backbone, we completely remove the backbone network within the GLAFF and map the future using only timestamps. Surprisingly, GLAFF still demonstrates favorable prediction performance without any observations. The average prediction accuracy of GLAFF even outperforms Informer and DLinear, and is also competitive with TimesNet and iTransformer. Global information proves adequate in scenarios featuring clear periodic and stable distributions.

In w/o Attention, we substitute the stacked attention blocks with MLP networks having the equivalent size. Following the replacement of attention blocks, GLAFF fails to capture the dependencies among timestamps adequately. It proves challenging to map out precise observations solely from a single timestamp. Particularly notable is the most marked decline in performance on the Traffic dataset, which has the largest number of channels, indicating the greatest modeling challenge for GLAFF.

In w/o Quantile, we replace the Robust Denormalizer with conventional inverse normalization. The experimental results illustrate that our design yields enhancements across all three datasets, particularly in the Electricity dataset. When the history window encompasses anomalies, conventional inverse normalization yields inaccurate estimates for distribution. Leveraging more robust quantiles, our Robust Denormalizer demonstrates enhanced robustness in mitigating the impacts of data drift.

In w/o Adaptive, we substitute the Adaptive Combiner with a straightforward averaging for global mapping and local prediction. We distinctly find that dynamically adjusting the combined weights can prove more efficacious in accommodating fluctuating real-world scenarios, particularly evident in the non-stationary Weather dataset. By fusing global and local information adaptively, GLAFF can seamlessly collaborate with any time series forecasting backbone.

5 Conclusion

In this work, our focus lies in leveraging global information, as denoted by timestamps, to enhance the robust prediction capability of time series forecasting models in the real world. We introduce a new approach named GLAFF, serving as a model-agnostic and plug-and-play framework. Within this framework, the timestamps are modeled individually to capture the global dependencies. Through adaptive adjustment of combined weights for global and local information, GLAFF facilitates seamless collaboration with any time series forecasting backbone. To substantiate the superiority of our approach, we have conducted comprehensive experiments on widely used benchmark datasets, demonstrating the substantial enhancement GLAFF provides to mainstream forecasting models. We hope that GLAFF can be used as a foundational component for time series forecasting and call on the community to give more attention to global information represented by timestamps.

Acknowledgments and Disclosure of Funding

This work was supported by the National Natural Science Foundation of China under Grants (U23B2001, 62171057, 62101064, 62201072, 62001054, 62071067), the Ministry of Education and China Mobile Joint Fund (MCM20200202, MCM20180101), Beijing University of Posts and Telecommunications-China Mobile Research Institute Joint Innovation Center, China Postdoctoral Science Foundation (2023TQ0039), National Postdoctoral Program for Innovative Talents under Grant BX20230052, and the BUPT Excellent Ph.D. Students Foundation (CX20241016).

References

- [1] Adebiyi Ariyo Ariyo, Aderemi Oluyinka Adewumi, and Charles K. Ayo. Stock price prediction using the ARIMA model. In *International Conference on Computer Modelling and Simulation*, pages 106–112, 2014.
- [2] G. E. P. Box and G. M. Jenkins. Some recent advances in forecasting and control. *Journal of the Royal Statistical Society*, 17:91–109, 1968.
- [3] Ching Chang, Wen-Chih Peng, and Tien-Fu Chen. LLM4TS: two-stage fine-tuning for time-series forecasting with pre-trained llms. *arXiv*, 2308.08469, 2023.
- [4] Yuzhou Chen, Ignacio Segovia-Dominguez, Baris Coskunuzer, and Yulia R. Gel. Tamps2gcnets: Coupling time-aware multipersistence knowledge representation with spatio-supra graph convolutional networks for time-series forecasting. In *International Conference on Learning Representations*, 2022.
- [5] Hao Cheng, Qingsong Wen, Yang Liu, and Liang Sun. Robusttsf: Towards theory and design of robust time series forecasting with anomalies. In *International Conference on Learning Representations*, 2024.
- [6] Ailin Deng and Bryan Hooi. Graph neural network-based anomaly detection in multivariate time series. In *AAAI Conference on Artificial Intelligence*, pages 4027–4035, 2021.
- [7] Jiaxiang Dong, Haixu Wu, Haoran Zhang, Li Zhang, Jianmin Wang, and Mingsheng Long. Simmtm: A simple pre-training framework for masked time-series modeling. In *Annual Conference on Neural Information Processing Systems*, 2023.
- [8] Shengdong Du, Tianrui Li, Yan Yang, and Shi-Jinn Horng. Deep air quality forecasting using hybrid deep learning framework. *IEEE Transactions on Knowledge and Data Engineering*, 33:2412–2424, 2021.
- [9] Wei Fan, Pengyang Wang, Dongkun Wang, Dongjie Wang, Yuanchun Zhou, and Yanjie Fu. Dish-ts: A general paradigm for alleviating distribution shift in time series forecasting. In *AAAI Conference on Artificial Intelligence*, pages 7522–7529, 2023.
- [10] Valentin Flunkert, David Salinas, and Jan Gasthaus. Deepar: Probabilistic forecasting with autoregressive recurrent networks. *arXiv*, 2201.00382, 2017.
- [11] Hui He, Qi Zhang, Simeng Bai, Kun Yi, and Zhendong Niu. CATN: cross attentive tree-aware network for multivariate time series forecasting. In *AAAI Conference on Artificial Intelligence*, pages 4030–4038, 2022.
- [12] Qi-Qiao He, Shirley Weng In Siu, and Yain-Whar Si. Instance-based deep transfer learning with attention for stock movement prediction. *Applied Intelligence*, 53:6887–6908, 2023.
- [13] Sepp Hochreiter and Jürgen Schmidhuber. Long short-term memory. *Neural Computation*, 9:1735–1780, 1997.
- [14] Rob J Hyndman and George Athanasopoulos. *Forecasting: Principles and Practice*. OTexts, 2018.
- [15] Yuxin Jia, Youfang Lin, Xinyan Hao, Yan Lin, Shengnan Guo, and Huaiyu Wan. WITRAN: water-wave information transmission and recurrent acceleration network for long-range time series forecasting. In *Annual Conference on Neural Information Processing Systems*, 2023.

[16] Shruti Kaushik, Abhinav Choudhury, Pankaj Kumar Sheron, Nataraj Dasgupta, Sayee Natarajan, Larry A. Pickett, and Varun Dutt. AI in healthcare: Time-series forecasting using statistical, neural, and ensemble architectures. *Frontiers Big Data*, 3:4, 2020.

[17] Taesung Kim, Jinhee Kim, Yunwon Tae, Cheonbok Park, Jang-Ho Choi, and Jaegul Choo. Reversible instance normalization for accurate time-series forecasting against distribution shift. In *International Conference on Learning Representations*, 2022.

[18] Nikita Kitaev, Lukasz Kaiser, and Anselm Levskaya. Reformer: The efficient transformer. In *International Conference on Learning Representations*, 2020.

[19] Shiyang Li, Xiaoyong Jin, Yao Xuan, Xiyou Zhou, Wenhui Chen, Yu-Xiang Wang, and Xifeng Yan. Enhancing the locality and breaking the memory bottleneck of transformer on time series forecasting. In *Annual Conference on Neural Information Processing Systems*, pages 5244–5254, 2019.

[20] Paul Pu Liang, Amir Zadeh, and Louis-Philippe Morency. Foundations & trends in multimodal machine learning: Principles, challenges, and open questions. *ACM Computing Surveys*, 56:264, 2024.

[21] Minhao Liu, Ailing Zeng, Muxi Chen, Zhijian Xu, Qiuxia Lai, Lingna Ma, and Qiang Xu. Scinet: Time series modeling and forecasting with sample convolution and interaction. In *Annual Conference on Neural Information Processing Systems*, 2022.

[22] Shizhan Liu, Hang Yu, Cong Liao, Jianguo Li, Weiyao Lin, Alex X. Liu, and Schahram Dustdar. Pyraformer: Low-complexity pyramidal attention for long-range time series modeling and forecasting. In *International Conference on Learning Representations*, 2022.

[23] Yong Liu, Haixu Wu, Jianmin Wang, and Mingsheng Long. Non-stationary transformers: Exploring the stationarity in time series forecasting. In *Annual Conference on Neural Information Processing Systems*, 2022.

[24] Yong Liu, Tengge Hu, Haoran Zhang, Haixu Wu, Shiyu Wang, Lintao Ma, and Mingsheng Long. itransformer: Inverted transformers are effective for time series forecasting. In *International Conference on Learning Representations*, 2024.

[25] Zhiding Liu, Mingyue Cheng, Zhi Li, Zhenya Huang, Qi Liu, Yanhu Xie, and Enhong Chen. Adaptive normalization for non-stationary time series forecasting: A temporal slice perspective. In *Annual Conference on Neural Information Processing Systems*, 2023.

[26] Yuqi Nie, Nam H. Nguyen, Phanwadee Sinthong, and Jayant Kalagnanam. A time series is worth 64 words: Long-term forecasting with transformers. In *International Conference on Learning Representations*, 2023.

[27] Luis Manuel Pereira, Addisson Salazar, and Luis Vergara. A comparative analysis of early and late fusion for the multimodal two-class problem. *IEEE Access*, 11:84283–84300, 2023.

[28] Tiago Pinto, Isabel Praça, Zita A. Vale, and José Silva. Ensemble learning for electricity consumption forecasting in office buildings. *Neurocomputing*, 423:747–755, 2021.

[29] Chetanya Puri, Gerben Kooijman, Bart Vanrumste, and Stijn Luca. Forecasting time series in healthcare with gaussian processes and dynamic time warping based subset selection. *IEEE Journal of Biomedical and Health Informatics*, 26:6126–6137, 2022.

[30] Syama Sundar Rangapuram, Matthias W. Seeger, Jan Gasthaus, Lorenzo Stella, Yuyang Wang, and Tim Januschowski. Deep state space models for time series forecasting. In *Annual Conference on Neural Information Processing Systems*, pages 7796–7805, 2018.

[31] Tárik S. Salem, Karan Kathuria, Heri Ramampiaro, and Helge Langseth. Forecasting intra-hour imbalances in electric power systems. In *AAAI Conference on Artificial Intelligence*, pages 9595–9600, 2019.

[32] Chenxi Sun, Yaliang Li, Hongyan Li, and Shenda Hong. TEST: text prototype aligned embedding to activate llm’s ability for time series. In *International Conference on Learning Representations*, 2024.

- [33] Sean J. Taylor and Benjamin Letham. Forecasting at scale. *PeerJ PrePrints*, 5:e3190, 2017.
- [34] Ashish Vaswani, Noam Shazeer, Niki Parmar, Jakob Uszkoreit, Llion Jones, Aidan N. Gomez, Łukasz Kaiser, and Illia Polosukhin. Attention is all you need. In *Annual Conference on Neural Information Processing Systems*, pages 5998–6008, 2017.
- [35] Chengsen Wang, Zirui Zhuang, Qi Qi, Jingyu Wang, Xingyu Wang, Haifeng Sun, and Jianxin Liao. Drift doesn’t matter: Dynamic decomposition with diffusion reconstruction for unstable multivariate time series anomaly detection. In *Annual Conference on Neural Information Processing Systems*, 2023.
- [36] Huiqiang Wang, Jian Peng, Feihu Huang, Jince Wang, Junhui Chen, and Yifei Xiao. MICN: multi-scale local and global context modeling for long-term series forecasting. In *International Conference on Learning Representations*, 2023.
- [37] Haixu Wu, Jiehui Xu, Jianmin Wang, and Mingsheng Long. Autoformer: Decomposition transformers with auto-correlation for long-term series forecasting. In *Annual Conference on Neural Information Processing Systems*, pages 22419–22430, 2021.
- [38] Haixu Wu, Tengge Hu, Yong Liu, Hang Zhou, Jianmin Wang, and Mingsheng Long. Timesnet: Temporal 2d-variation modeling for general time series analysis. In *International Conference on Learning Representations*, 2023.
- [39] Kun Yi, Qi Zhang, Wei Fan, Hui He, Liang Hu, Pengyang Wang, Ning An, Longbing Cao, and Zhendong Niu. Fouriergnn: Rethinking multivariate time series forecasting from a pure graph perspective. In *Annual Conference on Neural Information Processing Systems*, 2023.
- [40] Kun Yi, Qi Zhang, Wei Fan, Shoujin Wang, Pengyang Wang, Hui He, Ning An, Defu Lian, Longbing Cao, and Zhendong Niu. Frequency-domain mlps are more effective learners in time series forecasting. In *Annual Conference on Neural Information Processing Systems*, 2023.
- [41] Ailing Zeng, Muxi Chen, Lei Zhang, and Qiang Xu. Are transformers effective for time series forecasting? In *AAAI Conference on Artificial Intelligence*, pages 11121–11128, 2023.
- [42] Yifan Zhang, Qingsong Wen, Xue Wang, Weiqi Chen, Liang Sun, Zhang Zhang, Liang Wang, Rong Jin, and Tieniu Tan. Onenet: Enhancing time series forecasting models under concept drift by online ensembling. In *Annual Conference on Neural Information Processing Systems*, 2023.
- [43] Yunhao Zhang and Junchi Yan. Crossformer: Transformer utilizing cross-dimension dependency for multivariate time series forecasting. In *International Conference on Learning Representations*, 2023.
- [44] Yu Zheng, Xiuwen Yi, Ming Li, Ruiyuan Li, Zhangqing Shan, Eric Chang, and Tianrui Li. Forecasting fine-grained air quality based on big data. In *ACM SIGKDD International Conference on Knowledge Discovery and Data Mining*, pages 2267–2276, 2015.
- [45] Haoyi Zhou, Shanghang Zhang, Jieqi Peng, Shuai Zhang, Jianxin Li, Hui Xiong, and Wancai Zhang. Informer: Beyond efficient transformer for long sequence time-series forecasting. In *AAAI Conference on Artificial Intelligence*, pages 11106–11115, 2021.
- [46] Tian Zhou, Ziqing Ma, Qingsong Wen, Xue Wang, Liang Sun, and Rong Jin. Fedformer: Frequency enhanced decomposed transformer for long-term series forecasting. In *International Conference on Machine Learning*, pages 27268–27286, 2022.
- [47] Tian Zhou, Peisong Niu, Xue Wang, Liang Sun, and Rong Jin. One fits all: Power general time series analysis by pretrained LM. In *Annual Conference on Neural Information Processing Systems*, 2023.

A Detailed Experimental Setup

A.1 Dataset

We conduct extensive experiments on nine real-world datasets across five domains, including Electricity, Exchange, Traffic, Weather, and ILI, along with four ETT datasets. Table 4 summarizes the statistics of these datasets. These datasets have been widely utilized for benchmarking purposes and are publicly available. (1) **Electricity**⁴ comprises hourly electricity consumption for 321 customers from 2012 to 2014. (2) **Exchange**⁵ encompasses panel data on daily exchange rates for 8 countries from 1990 to 2019. (3) **Traffic**⁶ aggregates hourly road occupancy rates measured by 862 sensors on San Francisco Bay Area freeways from 2015 to 2016. (4) **Weather**⁷ captures 21 weather parameters monitored every 10 minutes from Germany in 2020. (5) **ILI**⁸ records the percentage of patients with influenza-like illness and the total number of such patients collected weekly by the United States Centers for Disease Control and Prevention from 2002 to 2020. (6) **ETT**⁹ records the oil temperature and load characteristics of two power transformers from 2016 to 2018, each at 2 different resolutions (15 minutes and 1 hour), resulting in a total of four datasets: ETTm1, ETTm2, ETTh1, and ETTh2.

Table 4: The statistics of each dataset. Channel represents the variate number of each dataset. Length indicates the total number of time points. Frequency denotes the sampling interval of time points.

Dataset	Channel	Length	Frequency	Information
Electricity	321	26304	1 Hour	Energy
Exchange	8	7588	1 Day	Finance
Traffic	862	17544	1 Hour	Transportation
Weather	21	52696	10 Minutes	Climate
ILI	7	966	1 Week	Healthcare
ETTh1 & ETTh2	7	17420	1 Hour	Energy
ETTm1 & ETTm2	7	69680	15 Minutes	Energy

A.2 Backbone

To demonstrate the effectiveness of our framework, we select several mainstream forecasting models based on different architectures, including the Transformer-based Informer (2021) and iTransformer (2024), the Linear-based DLinear (2023), and the Convolution-based TimesNet (2023). All aforementioned models are non-autoregressive forecasting models. (1) **Informer**¹⁰ utilizes the ProbSparse attention and distillation mechanism to manage exceedingly long input sequences efficiently and incorporates a generative decoder to mitigate the error accumulation inherent in autoregressive forecasting methodologies. (2) **DLinear**¹¹ employs decomposition-enhanced simple linear networks to attain competitive forecasting performance. (3) **TimesNet**¹² accurately models two-dimensional dependencies by transforming the one-dimensional time series into a collection of two-dimensional tensors, leveraging multiple periods to embed intra-periodic and inter-periodic variations along the columns and rows of the tensor, respectively. (4) **iTransformer**¹³ embeds individual channel into token employed by the attention mechanism, facilitating the capture of inter-channel multivariate correlations while applying a feed-forward network to each token to acquire nonlinear representations.

All backbones are based on our runs, using the same hardware. We utilize official or open-source implementations and follow the hyperparameter configurations recommended in their papers.

⁴<https://archive.ics.uci.edu/dataset/321/electricityloaddiagrams20112014>

⁵<https://github.com/laiguokun/multivariate-time-series-data>

⁶<https://pems.dot.ca.gov>

⁷<https://www.bgc-jena.mpg.de/wetter>

⁸<https://gis.cdc.gov/grasp/fluvview/fluportaldashboard.html>

⁹<https://github.com/zhouhaoyi/ETDataset>

¹⁰<https://github.com/zhouhaoyi/Informer2020>

¹¹<https://github.com/cure-lab/LTSF-Linear>

¹²<https://github.com/thuml/TimesNet>

¹³<https://github.com/thuml/ITransformer>

Algorithm 1 GLAFF

```
import torch
from torch import nn

class GLAFF(nn.Module):
    def __init__(self, hist_len, channel, dim=512, dff=2048, dropout=0.1, head_num=8, layer_num=2):
        """
        :param hist_len: the length of the history window
        :param channel: the number of the dataset channel
        :param dim: the dimension of the MultiHeadAttention
        :param dff: the dimension of the feedforward network
        :param dropout: the dropout proportion of the MultiHeadAttention
        :param head_num: the number of the attention head in the MultiHeadAttention
        :param layer_num: the number of the attention block in the Attention-based Mapper
        """

        super(GLAFF, self).__init__()

        self.Mapper = nn.Sequential(
            nn.Linear(6, dim),
            nn.TransformerEncoder(
                nn.TransformerEncoderLayer(
                    d_model=dim,
                    nhead=head_num,
                    dim_feedforward=dff,
                    dropout=dropout,
                    activation='gelu',
                    batch_first=True,
                ),
                num_layers=layer_num,
                norm=nn.LayerNorm(dim)
            ),
            nn.Linear(dim, channel)
        )

        self.Combiner = nn.Sequential(
            nn.Linear(hist_len, dff),
            nn.GELU(),
            nn.Linear(dff, 2),
            nn.Softmax(dim=-1)
        )

    def forward(self, hist_gt, hist_ts, pred_pr, pred_ts, q=0.75):
        """
        :param hist_gt: the true value in the history window
        :param hist_ts: the timestamps in the history window
        :param pred_pr: the prediction value of the backbone in the prediction window
        :param pred_ts: the timestamps in the prediction window
        :param q: the quantile of the Robust Denormalizer
        """

        # map
        hist_map = self.Mapper(hist_ts) # the mapping value of the mapper in the history window
        pred_map = self.Mapper(pred_ts) # the mapping value of the mapper in the prediction window

        # inverse normalize
        scale_gt = torch.quantile(hist_gt, q, 1, True) - torch.quantile(hist_gt, 1 - q, 1, True)
        scale_map = torch.quantile(hist_map, q, 1, True) - torch.quantile(hist_map, 1 - q, 1, True)
        stdev = scale_gt / scale_map
        means = torch.median(hist_gt - hist_map * stdev, dim=1, keepdim=True)[0]
        hist_map = hist_map * stdev + means
        pred_map = pred_map * stdev + means

        # combine
        error = hist_gt - hist_map
        weight = self.Combiner(error.permute(0, 2, 1)).unsqueeze(1)
        pred = torch.stack([pred_map, pred_pr], dim=-1)
        pred = torch.sum(pred * weight, dim=-1)

        return pred, hist_map, pred_map
```

A.3 Implementation

We employ the Adam optimizer and L_2 loss for model optimization, initializing the learning rate at 10^{-4} . The batch size is uniformly set to 32, and the number of training epochs is fixed at 10. Optimal hyperparameters for GLAFF are determined through grid search, employing a common setup shared across all datasets and backbones. The number l of the attention blocks in the Attention-based Mapper is designated as 2 (selected from $\{1,2,3,4,5\}$), and while proportion p of dropout is set to 0.1 (selected from $\{0.0,0.1,0.2,0.3,0.4\}$). The quantile q in the Robust Denormalizer is configured to 0.75, selected from $\{0.55, 0.65, 0.75, 0.85, 0.95\}$. We provide details of each hyperparameter in

Appendix B.3. All experiments are conducted using Python 3.10.13 and PyTorch 2.1.2, executed on an Ubuntu server equipped with an AMD Ryzen 9 7950X 16-Core processor and a single NVIDIA GeForce RTX 4090 graphics card, with each experiment repeated three times using different random seeds. If not explicitly stated, we report the Mean Square Error (MSE) and Mean Absolute Error (MAE) as evaluation metrics, with lower values indicating superior performance.

The detailed implementation of GLAFF is delineated in Algorithm 1. For simplification, the Adaptive Combiner is implemented through a straightforward two-layer linear network. We employ the *nn.TransformerEncoder()* within PyTorch to realize the Attention-based Mapper. The source code and checkpoints have been made openly accessible to facilitate future research.

B Full Experimental Result

B.1 Robustness Analysis

We report in Table 5 the means and standard deviations of the evaluation metrics for the baselines and GLAFF under three runs using different random seeds, facilitating the assessment of their robustness in long-range and ultra-long-range time series forecasting tasks. Evident from the mean of the experimental outcomes, GLAFF consistently demonstrates marked superiority over all four mainstream forecasting models across all nine real-world benchmark datasets. The standard deviation indicates the consistent stability and robustness of our proposed framework.

B.2 Ablation Study

We provide a comprehensive ablation study to validate the necessity of the GLAFF components. We implement our approach and its four variants on the iTransformer backbone. Specifically, in w/o Backbone, we completely remove the backbone network within the GLAFF and map the future using only timestamps. In w/o Attention, we substitute the stacked attention blocks with MLP networks having the equivalent size. In w/o Quantile, we replace the Robust Denormalizer with conventional inverse normalization. In w/o Adaptive, we substitute the Adaptive Combiner with a straightforward averaging mechanism for global mapping and local prediction. Due to space limitations, Section 4.4 presents experimental results for only three representative datasets, so we provide the complete results for nine real-world datasets in also Table 6.

When excluding any observations within the history window, GLAFF demonstrates an average prediction accuracy superior to Informer across nine real-world datasets and remains competitive with DLinear. However, in contrast to the three representative datasets outlined in Section 4.4, the average prediction accuracy of GLAFF across the nine datasets still lags behind TimesNet and iTransformer. We find that this discrepancy primarily stems from the highly non-stationary ILI dataset. In highly non-stationary scenarios, relying solely on global information fails to adapt to the intricate and fluctuating nature of real-world conditions. Our experimental outcomes validate the indispensable nature of both the robustness of global information and the flexibility of local information for accurate time series prediction.

The experimental results show that the adaptive adjustment of combined weights within the Adaptive Combiner is the most important among various designs. When the time series pattern exhibits clarity and stability, greater emphasis should be placed on robust global information. Conversely, increased attention should be directed towards flexible local information when the time series pattern appears ambiguous and variable. By fusing global and local information adaptively, GLAFF can seamlessly collaborate with any time series forecasting backbone to adapt to intricate and fluctuating real-world scenarios. Furthermore, the stacked attention blocks within the Attention-based Mapper and the robust inverse normalization within the Robust Denormalizer also yield notable contributions to enhancing the forecasting performance of GLAFF through efficient modeling of timestamps and robust mitigation of data drift.

It is noteworthy that the lack of either component design will corrupt the outcome of the GLAFF, resulting in a prediction accuracy lower than the standard iTransformer baseline. This aligns with both common knowledge and theoretical expectations. In terms of global information, the introduction of insufficient (w/o Attention), inaccurate (w/o Quantile), or crude (w/o Adaptive) will all hurt GLAFF. This again validates that each component design in GLAFF is reasonable and necessary.

Table 5: The complete forecasting errors for multivariate time series among GLAFF and mainstream baselines. A lower outcome indicates a better prediction. The best results are highlighted in bold.

Method	Informer				+ Ours				DLinear				+ Ours			
	MSE	MAE	MSE	MAE	MSE	MAE	MSE	MAE	MSE	MAE	MSE	MAE	MSE	MAE	MSE	MAE
Electricity	96	0.3328±0.0053	0.4138±0.0007	0.2173±0.0007	0.3232±0.0007	0.1962±0.0001	0.2830±0.0005	0.1470±0.0008	0.2378±0.0011							
	192	0.3623±0.0274	0.4444±0.0244	0.2201±0.0027	0.3292±0.0034	0.1962±0.0001	0.2861±0.0003	0.1715±0.0039	0.2530±0.0010							
	336	0.3519±0.0026	0.4342±0.0014	0.2302±0.0015	0.3374±0.0024	0.2080±0.0000	0.3008±0.0003	0.1965±0.0114	0.2736±0.0050							
	720	0.3640±0.0179	0.4427±0.0147	0.2472±0.0017	0.3507±0.0003	0.2392±0.0002	0.3305±0.0005	0.2390±0.0076	0.3082±0.0036							
ETTh1	96	0.9255±0.0694	0.7361±0.0367	0.6088±0.0157	0.5688±0.0071	0.4085±0.0004	0.4399±0.0002	0.3909±0.0099	0.4181±0.0097							
	192	1.2354±0.0679	0.8437±0.0146	0.8312±0.0976	0.6797±0.0474	0.4572±0.0006	0.4752±0.0003	0.4462±0.0108	0.4565±0.0083							
	336	1.3541±0.0747	0.8754±0.0107	0.8816±0.0249	0.6978±0.0033	0.5002±0.0005	0.5064±0.0011	0.4922±0.0040	0.4879±0.0021							
	720	1.2641±0.0292	0.8572±0.0101	0.9366±0.0367	0.7301±0.0199	0.6098±0.0012	0.5757±0.0001	0.6088±0.0028	0.5560±0.0011							
ETTh2	96	0.7083±0.0800	0.5493±0.0301	0.4219±0.0393	0.4427±0.0186	0.1589±0.0006	0.2776±0.0013	0.1282±0.0051	0.2049±0.0055							
	192	1.1329±0.1858	0.6879±0.0493	0.8599±0.0622	0.5994±0.0343	0.1869±0.0025	0.3091±0.0028	0.1651±0.0135	0.2382±0.0068							
	336	0.9972±0.1608	0.6666±0.0601	0.7471±0.1531	0.5702±0.0558	0.2066±0.0021	0.3304±0.0025	0.2064±0.0249	0.2650±0.0077							
	720	1.6066±0.3017	0.8152±0.0768	1.2550±0.0489	0.7203±0.0270	0.2621±0.0026	0.3783±0.0021	0.2135±0.0079	0.2875±0.0064							
ETTm1	96	0.5932±0.0320	0.5475±0.0126	0.5031±0.0060	0.4862±0.0026	0.3385±0.0003	0.3877±0.0006	0.3085±0.0230	0.3529±0.0130							
	192	0.6111±0.0117	0.5763±0.0038	0.5339±0.0191	0.5248±0.0074	0.3936±0.0007	0.4179±0.0007	0.3619±0.0071	0.3857±0.0058							
	336	0.8881±0.0376	0.7257±0.0206	0.7066±0.0932	0.6278±0.0387	0.4502±0.0009	0.4514±0.0004	0.4416±0.0208	0.4320±0.0090							
	720	1.0374±0.0480	0.7859±0.0104	0.9254±0.0230	0.7185±0.0099	0.5075±0.0010	0.4932±0.0010	0.4930±0.0068	0.4669±0.0026							
ETTm2	96	0.1860±0.0089	0.3109±0.0103	0.1473±0.0303	0.2656±0.0279	0.1148±0.0003	0.2318±0.0012	0.0803±0.0010	0.1649±0.0020							
	192	0.2421±0.0286	0.3481±0.0229	0.2300±0.0457	0.3405±0.0351	0.1425±0.0002	0.2605±0.0005	0.1085±0.0024	0.1932±0.0036							
	336	0.4542±0.0614	0.4664±0.0287	0.3082±0.0022	0.3798±0.0076	0.1760±0.0012	0.2939±0.0019	0.1477±0.0027	0.2292±0.0036							
	720	0.8609±0.2400	0.6156±0.0665	0.7192±0.0489	0.5611±0.0174	0.2252±0.0010	0.3396±0.0011	0.2211±0.0483	0.2737±0.0080							
Exchange	96	0.7349±0.0501	0.7282±0.0226	0.2226±0.0059	0.3905±0.0042	0.0505±0.0005	0.1642±0.0013	0.0462±0.0004	0.1552±0.0007							
	192	1.0158±0.0258	0.8607±0.0146	0.4214±0.0237	0.5471±0.0147	0.0988±0.0006	0.2375±0.0013	0.0929±0.0015	0.2247±0.0022							
	336	1.3307±0.0715	0.9708±0.0177	0.6912±0.0292	0.6939±0.0150	0.1739±0.0038	0.3170±0.0039	0.1612±0.0028	0.2993±0.0038							
	720	2.0536±0.0518	1.2631±0.0132	1.1516±0.0718	0.9222±0.0254	0.3137±0.0018	0.4460±0.0004	0.3077±0.0019	0.4386±0.0039							
ILJ	24	3.3735±0.1341	1.3561±0.0583	2.4865±0.1512	1.1055±0.0405	2.0871±0.0224	1.1314±0.0037	1.8745±0.0541	0.9629±0.0193							
	36	3.0944±0.0858	1.2927±0.0999	2.6173±0.1699	1.1570±0.0638	2.0654±0.0323	1.1074±0.0077	1.7557±0.0834	0.9571±0.0201							
	48	3.3828±0.0680	1.3701±0.0308	2.8792±0.0996	1.2296±0.0415	2.0586±0.0133	1.0879±0.0040	1.6393±0.0430	0.9115±0.0166							
	60	3.6102±0.1638	1.4147±0.0313	3.0858±0.1401	1.2743±0.0478	2.1861±0.0212	1.0969±0.0039	1.6441±0.0333	0.8894±0.0124							
Traffic	96	0.4668±0.0265	0.3748±0.0150	0.3521±0.0125	0.2969±0.0087	0.4821±0.0001	0.3782±0.0001	0.3007±0.0006	0.2602±0.0011							
	192	0.4549±0.0043	0.3713±0.0031	0.3430±0.0094	0.2882±0.0056	0.4487±0.0001	0.3561±0.0003	0.3019±0.0036	0.2609±0.0021							
	336	0.4622±0.0088	0.3778±0.0054	0.3352±0.0009	0.2812±0.0023	0.4526±0.0001	0.3577±0.0002	0.3062±0.0011	0.2631±0.0002							
	720	0.4945±0.0106	0.3997±0.0073	0.3403±0.0166	0.2870±0.0101	0.4749±0.0001	0.3735±0.0002	0.3267±0.0028	0.2776±0.0013							
Weather	96	1.4216±0.2777	0.8670±0.0771	0.6420±0.0319	0.5535±0.0118	0.1975±0.0013	0.2577±0.0030	0.1758±0.0023	0.2435±0.0038							
	192	1.4292±0.3063	0.8800±0.0936	0.8767±0.0966	0.6636±0.0304	0.2371±0.0005	0.2963±0.0010	0.2194±0.0041	0.2795±0.0013							
	336	1.7964±0.6657	1.0076±0.1761	1.5063±0.1426	0.8511±0.0366	0.2819±0.0005	0.3331±0.0009	0.2652±0.0088	0.3121±0.0038							
	720	1.5424±0.0315	0.9457±0.0208	1.4271±0.0529	0.8531±0.0099	0.3427±0.0004	0.3794±0.0002	0.3297±0.0010	0.3596±0.0006							
TimesNet	24	0.2799±0.0002	0.1541±0.0016	0.2475±0.0019		0.1525±0.0001	0.2460±0.0004	0.1197±0.0035	0.1979±0.0006							
	36	0.1908±0.0043	0.2933±0.0038	0.1694±0.0017	0.2608±0.0018	0.1674±0.0003	0.2593±0.0007	0.1434±0.0009	0.2157±0.0011							
	48	0.2112±0.0094	0.3104±0.0075	0.1850±0.0041	0.2762±0.0039	0.1830±0.0018	0.2762±0.0016	0.1683±0.0023	0.2395±0.0017							
	60	0.2353±0.0063	0.3257±0.0028	0.2260±0.0112	0.3027±0.0033	0.2199±0.0007	0.3097±0.0010	0.2169±0.0039	0.2786±0.0005							
ETTh1	96	0.4534±0.0095	0.4811±0.0054	0.4349±0.0055	0.4643±0.0027	0.4200±0.0039	0.4536±0.0038	0.4112±0.0017	0.4407±0.0014							
	192	0.5331±0.0019	0.5308±0.0054	0.5195±0.0103	0.5170±0.0066	0.4944±0.0111	0.5020±0.0059	0.4739±0.0039	0.4816±0.0021							
	336	0.6209±0.0027	0.5796±0.0013	0.5961±0.0014	0.5598±0.0014	0.5382±0.0035	0.5276±0.0029	0.5336±0.0033	0.5188±0.0031							
	720	0.8444±0.0717	0.6968±0.0313	0.7730±0.0163	0.6605±0.0047	0.7159±0.0157	0.6293±0.0069	0.7040±0.0034	0.6153±0.0001							
ETTh2	96	0.1831±0.0028	0.2980±0.0012	0.1740±0.0064	0.2764±0.0035	0.1769±0.0039	0.2871±0.0017	0.1720±0.0040	0.2708±0.0013							
	192	0.2177±0.0020	0.3294±0.0030	0.2040±0.0036	0.3060±0.0017	0.1992±0.0019	0.3109±0.0021	0.1957±0.0029	0.2954±0.0028							
	336	0.2396±0.0026	0.3457±0.0008	0.2185±0.0033	0.3194±0.0033	0.2197±0.0060	0.3290±0.0038	0.2127±0.0008	0.3061±0.0023							
	720	0.2805±0.0103	0.3764±0.0030	0.2779±0.0137	0.3634±0.0117	0.2708±0.0140	0.3661±0.0105	0.2698±0.0132	0.3562±0.0094							
ETTm1	96	0.4493±0.0265	0.4477±0.0117	0.3805±0.0109	0.3983±0.0036	0.3832±0.0071	0.4145±0.0033	0.3489±0.0065	0.3856±0.0041							
	192	0.4478±0.0077	0.4608±0.0035	0.4400±0.0090	0.4315±0.0120	0.4285±0.0089	0.4451±0.0065	0.4034±0.0080	0.4201±0.0055							
	336	0.5502±0.0629	0.5041±0.0153	0.4944±0.0546	0.4616±0.0226	0.4851±0.0042	0.4794±0.0020	0.4680±0.0064	0.460							

Table 6: The complete forecasting errors for multivariate time series of ablation study among GLAFF and variants. A lower outcome indicates a better prediction. The best results are highlighted in bold.

Method	iTransformer				+ Ours		w/o Backbone		w/o Attention		w/o Quantile		w/o Adaptive	
	MSE	MAE	MSE	MAE	MSE	MAE	MSE	MAE	MSE	MAE	MSE	MAE	MSE	MAE
Electricity	96	0.1525	0.2460	0.1197	0.1979	0.2058	0.2663	0.1518	0.2450	0.1467	0.2465	0.1574	0.2502	
	192	0.1674	0.2593	0.1434	0.2157	0.2097	0.2793	0.1684	0.2610	0.1677	0.2662	0.1740	0.2662	
	336	0.1830	0.2762	0.1683	0.2395	0.2454	0.3014	0.1832	0.2775	0.1993	0.2954	0.1953	0.2877	
	720	0.2199	0.3097	0.2169	0.2786	0.2984	0.3386	0.2182	0.3092	0.2593	0.3403	0.2330	0.3171	
ETTh1	96	0.4200	0.4536	0.4112	0.4407	0.5741	0.5150	0.4282	0.4560	0.4230	0.4598	0.4590	0.4754	
	192	0.4944	0.5020	0.4739	0.4816	0.6422	0.5409	0.5166	0.5112	0.4861	0.5019	0.5427	0.5258	
	336	0.5382	0.5276	0.5336	0.5188	0.7020	0.5833	0.5797	0.5513	0.5496	0.5386	0.5836	0.5469	
	720	0.7159	0.6293	0.7040	0.6153	0.8481	0.6541	0.7564	0.6442	0.7065	0.6294	0.7429	0.6429	
ETTh2	96	0.1769	0.2871	0.1720	0.2708	0.2095	0.2786	0.1941	0.3270	0.1969	0.3308	0.2028	0.3337	
	192	0.1992	0.3109	0.1957	0.2954	0.2847	0.3274	0.2325	0.3618	0.2223	0.3562	0.2335	0.3631	
	336	0.2197	0.3290	0.2127	0.3061	0.2937	0.3384	0.2432	0.3722	0.2639	0.3896	0.2611	0.3848	
	720	0.2708	0.3661	0.2698	0.3562	0.3082	0.3567	0.2909	0.4051	0.2786	0.4036	0.3041	0.4197	
ETTm1	96	0.3832	0.4145	0.3489	0.3856	0.4161	0.4100	0.4106	0.4233	0.3595	0.4021	0.3841	0.4180	
	192	0.4285	0.4451	0.4034	0.4201	0.4932	0.4587	0.4547	0.4522	0.4138	0.4385	0.4397	0.4511	
	336	0.4851	0.4794	0.4680	0.4604	0.5467	0.4883	0.5278	0.4990	0.4797	0.4806	0.4984	0.4881	
	720	0.5660	0.5323	0.5636	0.5190	0.6210	0.5316	0.5942	0.5441	0.5814	0.5383	0.5883	0.5400	
ETTm2	96	0.1199	0.2347	0.1112	0.2205	0.1334	0.2340	0.1197	0.2337	0.1129	0.2293	0.1150	0.2296	
	192	0.1491	0.2656	0.1438	0.2517	0.1612	0.2624	0.1554	0.2677	0.1459	0.2627	0.1470	0.2614	
	336	0.1845	0.2933	0.1816	0.2829	0.1979	0.2901	0.1884	0.2944	0.1935	0.3006	0.1837	0.2924	
	720	0.2331	0.3334	0.2319	0.3267	0.2464	0.3272	0.2332	0.3297	0.2791	0.3627	0.2324	0.3306	
Exchange	96	0.0580	0.1719	0.0514	0.1580	0.0972	0.2212	0.0595	0.1748	0.0613	0.1771	0.0669	0.1870	
	192	0.1126	0.2447	0.1078	0.2306	0.1448	0.2779	0.1149	0.2475	0.1154	0.2470	0.1203	0.2539	
	336	0.2095	0.3391	0.1963	0.3144	0.2614	0.3772	0.2079	0.3371	0.2081	0.3359	0.2129	0.3404	
	720	0.5172	0.5505	0.5102	0.5291	0.6089	0.5952	0.5308	0.5582	0.5359	0.5605	0.5461	0.5668	
IL1	24	1.1477	0.6593	1.1289	0.6576	2.3361	1.0211	1.1321	0.6759	1.2641	0.6907	1.4264	0.7593	
	36	1.0608	0.6951	1.0391	0.6822	1.9812	0.9408	1.1258	0.7193	1.0839	0.7035	1.2890	0.7669	
	48	1.2094	0.7351	1.1637	0.7148	1.8142	0.9166	1.2250	0.7509	1.2472	0.7483	1.3530	0.7789	
	60	1.2223	0.7575	1.1956	0.7308	1.5257	0.8484	1.2615	0.7734	1.2239	0.7551	1.2319	0.7593	
Traffic	96	0.3084	0.2717	0.2828	0.2485	0.3348	0.2723	0.3172	0.2806	0.2909	0.2684	0.2930	0.2612	
	192	0.3267	0.2794	0.2909	0.2528	0.3387	0.2736	0.3357	0.2884	0.2948	0.2737	0.2970	0.2610	
	336	0.3381	0.2850	0.3005	0.2594	0.3460	0.2794	0.3482	0.2958	0.3023	0.2804	0.3082	0.2706	
	720	0.3574	0.3015	0.3201	0.2730	0.3558	0.2906	0.3684	0.3113	0.3249	0.2984	0.3212	0.2819	
Weather	96	0.1784	0.2229	0.1587	0.2199	0.2382	0.2695	0.1780	0.2214	0.1811	0.2270	0.1914	0.2379	
	192	0.2308	0.2675	0.2138	0.2654	0.2882	0.3105	0.2383	0.2733	0.2364	0.2768	0.2489	0.2832	
	336	0.2892	0.3099	0.2733	0.3058	0.3381	0.3414	0.2932	0.3146	0.2905	0.3134	0.3070	0.3251	
	720	0.3701	0.3634	0.3520	0.3547	0.4011	0.3813	0.3752	0.3664	0.3727	0.3649	0.3829	0.3722	
Avg.		0.3957	0.3875	0.3794	0.3689	0.5291	0.4278	0.4100	0.3987	0.4027	0.3971	0.4243	0.4036	

B.3 Hyperparameter Analysis

To assess the sensitivity of GLAFF for various hyperparameter configurations, we conduct a comprehensive hyperparameter analysis. It is worth noting that, in theory, GLAFF introduces only one additional core hyperparameter, the quantile q in the Robust Denormalizer. Therefore, conducting hyperparameter selection for GLAFF requires only very little work. However, to comprehensively compare the effects for different parameter configurations, we also explore the number l of attention blocks and the proportion p of dropout in the Attention-based Mapper. We implement our method on the iTransformer backbone. The length of the history window is fixed at 96, while the length of the prediction window is set to 192. The experimental results for the eight data-rich datasets are depicted in Figure 4.

The quantile in the Robust Denormalizer impacts the ability of GLAFF to adapt to data drift, particularly when anomalies are present within the sliding window. Higher quantiles can render GLAFF overly sensitive to magnitude, diminishing its robustness against outlier data. Conversely, smaller quantiles may hinder the ability of GLAFF to detect distribution changes, consequently impairing its capacity to adapt to data drift. For datasets ETTh1, ETTm1, and Traffic, higher quantiles correlate with increased prediction accuracy, while for datasets ETTh2 and Weather, lower quantiles yield higher prediction accuracy. Moreover, datasets ETTm2, Electricity, and Exchange demonstrate relative robustness to quantile variations. To equalize prediction accuracy, we adopt a quantile q of 0.75 for all datasets and backbones.

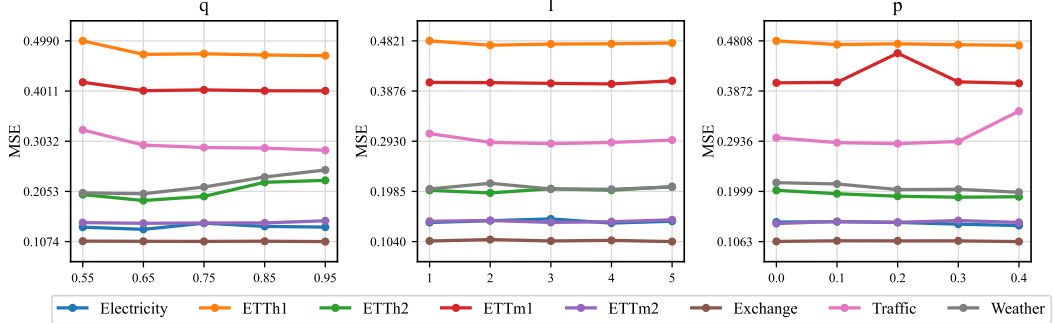


Figure 4: The forecasting errors for multivariate time series of hyperparameter analysis among different configurations for GLAFF. A lower outcome indicates a better prediction.

The number of attention blocks in the Attention-based Mapper influences the modeling process for global information representation. A greater depth in attention blocks enables GLAFF to model timestamp dependencies more sufficiently and uncover latent high-level semantic features. Nevertheless, augmenting the depth of the network also escalates computation costs and exacerbates convergence challenges. According to experimental findings, all benchmark datasets exhibit robustness to variations in the number l of attention blocks, thus facilitating the deployment of GLAFF. Considering training cost and model performance, we choose 2 as the number l of attention blocks for all datasets and backbones.

The proportion of dropout in the Attention-based Mapper impacts the generalization performance of GLAFF. When the dropout proportion is too small, indicating the retention of too many neurons, the model tends to overfit, thereby diminishing its generalization capacity. Conversely, if the dropout proportion is excessively large, meaning the exclusion of too many neurons, the model may struggle to effectively capture the underlying features, decreasing prediction accuracy. Moreover, a high dropout proportion can also impede the convergence of model training due to the varying network structures observed in each training sample. From the experimental results, except for the ETTm1 and Traffic datasets, most datasets exhibit insensitivity to the choice of dropout proportion p . To simplify the parameter selection challenge, we adopt a dropout proportion p of 0.1 for all datasets and backbones.

B.4 Efficiency Evaluation

To assess the practical applicability of GLAFF in real-world environments, we comprehensively compare training time and memory usage between baseline models and GLAFF across nine datasets. The experimental results are summarized in Table 7. Specifically, incorporating GLAFF results in an average 23.4382s increase in the training time and a 25.0608MB increase in memory usage. Presently, with hardware resources evolving rapidly, this computation costs may not affect the training and deployment of GLAFF in most scenarios, particularly when considering the significant accuracy enhancement it offers. Moreover, it is a common practice to trade off computation costs for enhanced prediction accuracy. For instance, the TimesNet baseline exhibits an average training time increase of 355s and an average memory cost increase of 145MB compared to the DLinear baseline, yielding a mere 8.4% increase in average prediction accuracy. In contrast, our GLAFF incurs a training time increase of 14s and a memory usage increase of 25MB while achieving a 13.1% increase in prediction accuracy compared to the DLinear backbone. In scenarios demanding high prediction accuracy, this computation costs are acceptable.

Notably, owing to the unique forecasting mechanism (mapping), the memory usage incurred by GLAFF remains insensitive to both the dataset and the prediction length, consistently hovering at approximately 25MB. Additionally, we observe that the introduction of GLAFF not only results in substantial enhancements in prediction accuracy in all scenarios, but also significantly reduces the training time in some scenarios (such as the TimesNet backbone on the ETTh2 dataset, the Informer backbone on the Traffic dataset, the DLinear backbone, and the TimesNet backbone). We postulate

Table 7: The training time and memory usage for multivariate time series forecasting among GLAFF and mainstream baselines. A lower outcome indicates a better efficiency.

Method	Informer + Ours				DLinear + Ours				TimesNet + Ours				iTransformer + Ours				
	Time (s)	Size (MB)	Time (s)	Size (MB)	Time (s)	Size (MB)	Time (s)	Size (MB)	Time (s)	Size (MB)	Time (s)	Size (MB)	Time (s)	Size (MB)	Time (s)	Size (MB)	
Electricity	96	15.92	67.05	17.63	92.52	5.701	0.071	8.226	25.54	86.18	146.2	100.5	171.6	27.71	48.48	31.49	73.95
	192	20.84	67.05	22.50	92.52	7.663	0.142	11.74	25.61	161.9	146.2	162.1	171.7	29.37	48.67	34.86	74.14
	336	29.05	67.05	31.40	92.52	10.58	0.249	17.49	25.72	396.2	146.3	279.5	171.7	31.82	48.95	40.43	74.42
	720	50.30	67.05	60.02	92.52	18.88	0.533	35.79	26.00	489.2	146.4	433.4	171.9	38.24	49.70	58.18	75.17
ETTh1	96	5.400	62.76	8.828	87.61	0.394	0.071	3.708	24.93	82.26	145.5	89.64	170.4	2.057	48.48	5.486	73.34
	192	6.195	62.76	11.55	87.61	0.447	0.142	5.528	25.00	137.5	145.6	169.0	170.4	2.107	48.67	7.191	73.53
	336	8.104	62.76	16.49	87.61	0.543	0.249	8.687	25.10	274.1	145.6	312.7	170.5	2.095	48.95	10.25	73.81
	720	12.78	62.76	30.18	87.61	0.727	0.533	18.44	25.39	336.6	145.8	314.0	170.6	2.269	49.70	19.81	74.56
ETTh2	96	5.605	62.76	8.833	87.61	0.405	0.071	3.740	24.93	98.52	145.5	105.6	170.4	1.945	48.48	5.476	73.34
	192	6.155	62.76	11.60	87.61	0.459	0.142	5.517	25.00	179.3	145.6	171.1	170.4	2.027	48.67	7.214	73.53
	336	8.125	62.76	16.51	87.61	0.535	0.249	8.702	25.10	375.4	145.6	221.7	170.5	2.084	48.95	10.30	73.81
	720	12.73	62.76	30.10	87.61	0.710	0.533	18.45	25.39	372.7	145.8	299.7	170.6	2.072	49.70	19.81	74.56
ETTm1	96	21.43	62.76	35.98	87.61	1.550	0.071	15.14	24.93	293.0	145.5	286.9	170.4	7.929	48.48	21.96	73.34
	192	25.07	62.76	47.45	87.61	1.833	0.142	22.47	25.00	382.0	145.6	556.5	170.4	8.737	48.67	29.40	73.53
	336	33.71	62.76	68.27	87.61	2.096	0.249	35.95	25.10	1017	145.6	1296	170.5	8.003	48.95	42.53	73.81
	720	54.73	62.76	129.8	87.61	3.099	0.533	79.09	25.39	1530	145.8	1405	170.6	8.719	49.70	84.83	74.56
ETTm2	96	21.83	62.76	35.44	87.61	1.553	0.071	15.11	24.93	306.7	145.5	308.4	170.4	8.144	48.48	22.09	73.34
	192	25.12	62.76	47.47	87.61	1.801	0.142	22.58	25.00	393.7	145.6	786.6	170.4	8.590	48.67	29.54	73.53
	336	33.41	62.76	68.43	87.61	2.126	0.249	35.93	25.10	1429	145.6	2631	170.5	8.318	48.95	42.44	73.81
	720	55.16	62.76	129.6	87.61	3.177	0.533	79.13	25.39	1499	145.8	1470	170.6	9.696	49.70	84.85	74.56
Exchange	96	2.242	62.77	3.823	87.63	0.173	0.071	1.600	24.93	32.51	145.5	37.20	170.4	0.865	48.48	2.336	73.34
	192	2.580	62.77	4.929	87.63	0.188	0.142	2.301	25.00	66.52	145.6	66.49	170.4	0.928	48.67	3.031	73.53
	336	3.340	62.77	6.752	87.63	0.218	0.249	3.543	25.11	159.0	145.6	209.2	170.5	0.859	48.95	4.209	73.81
	720	4.852	62.77	11.46	87.63	0.280	0.533	7.005	25.39	144.4	145.8	138.3	170.6	0.797	49.70	7.563	74.56
ILI	24	0.245	62.76	0.343	87.14	0.019	0.007	0.128	24.39	1.608	145.5	1.650	169.9	0.162	48.22	0.253	72.61
	36	0.244	62.76	0.326	87.14	0.019	0.010	0.129	24.40	1.664	145.5	1.717	169.9	0.146	48.25	0.252	72.63
	48	0.246	62.76	0.336	87.14	0.018	0.014	0.132	24.40	1.688	145.5	1.712	169.9	0.146	48.27	0.249	72.66
	60	0.248	62.76	0.354	87.14	0.019	0.017	0.143	24.40	1.769	145.5	1.701	169.9	0.141	48.30	0.270	72.68
Traffic	96	18.17	74.45	14.97	101.0	8.166	0.071	8.067	26.60	75.01	147.2	74.67	173.7	60.80	48.48	62.07	75.01
	192	25.29	74.45	19.77	101.0	12.17	0.142	11.49	26.67	131.2	147.3	102.1	173.8	63.71	48.67	64.85	75.20
	336	37.10	74.45	27.89	101.0	17.77	0.249	16.94	26.78	189.1	147.3	177.3	173.8	67.71	48.95	69.42	75.48
	720	65.19	74.45	49.28	101.0	31.00	0.533	32.11	27.06	266.4	147.5	286.0	174.0	77.75	49.70	82.50	76.23
Weather	96	16.69	62.95	27.68	87.83	1.645	0.071	11.71	24.95	208.8	145.6	274.0	170.5	6.877	48.48	17.06	73.37
	192	19.88	62.95	35.94	87.83	1.988	0.142	17.23	25.02	363.6	145.6	500.2	170.5	7.318	48.67	23.05	73.55
	336	26.84	62.95	51.92	87.83	2.472	0.249	27.46	25.13	653.6	145.7	743.1	170.5	7.614	48.95	32.99	73.84
	720	43.84	62.95	98.33	87.83	3.918	0.533	59.82	25.42	785.8	145.8	786.7	170.7	8.277	49.70	64.74	74.59

that this phenomenon can be attributed to the incorporation of global information, which accelerates the convergence of the network.

B.5 Prediction Showcase

In addition to evaluation metrics, forecasting quality is crucial. To comprehensively compare GLAFF and the four mainstream forecasting models, we present the complete prediction showcases for the nine real-world datasets in Figure 5. For the ILI dataset, the length of the history window is set to 36, while the length of the prediction window is set to 48. Except for the ILI dataset, the length of the history window is set to 96, and the length of the prediction window is set to 192. We can observe that by fusing the robustness of the global information and the flexibility of the local information, GLAFF demonstrates superior suitability for intricate and fluctuating real-world scenarios, thereby enhancing the ability of the backbone model to generate predictions that closely correspond to the ground truth.

C Broader Impact

The GLAFF proposed in our paper focuses on leveraging global information, as denoted by timestamps, to enhance the robust prediction capability of time series forecasting models in the real world. As a model-agnostic and plug-and-play module, GLAFF significantly improves mainstream forecasting models, positively influencing domains such as finance, transportation, energy, healthcare, climate, etc. Furthermore, GLAFF may inspire the community to give more attention to the utilization of global information and catalyze further development of time series forecasting techniques. The source code and checkpoints have been made publicly available to support future research. This paper only focuses on the algorithm design. Using all the codes and datasets strictly follows the

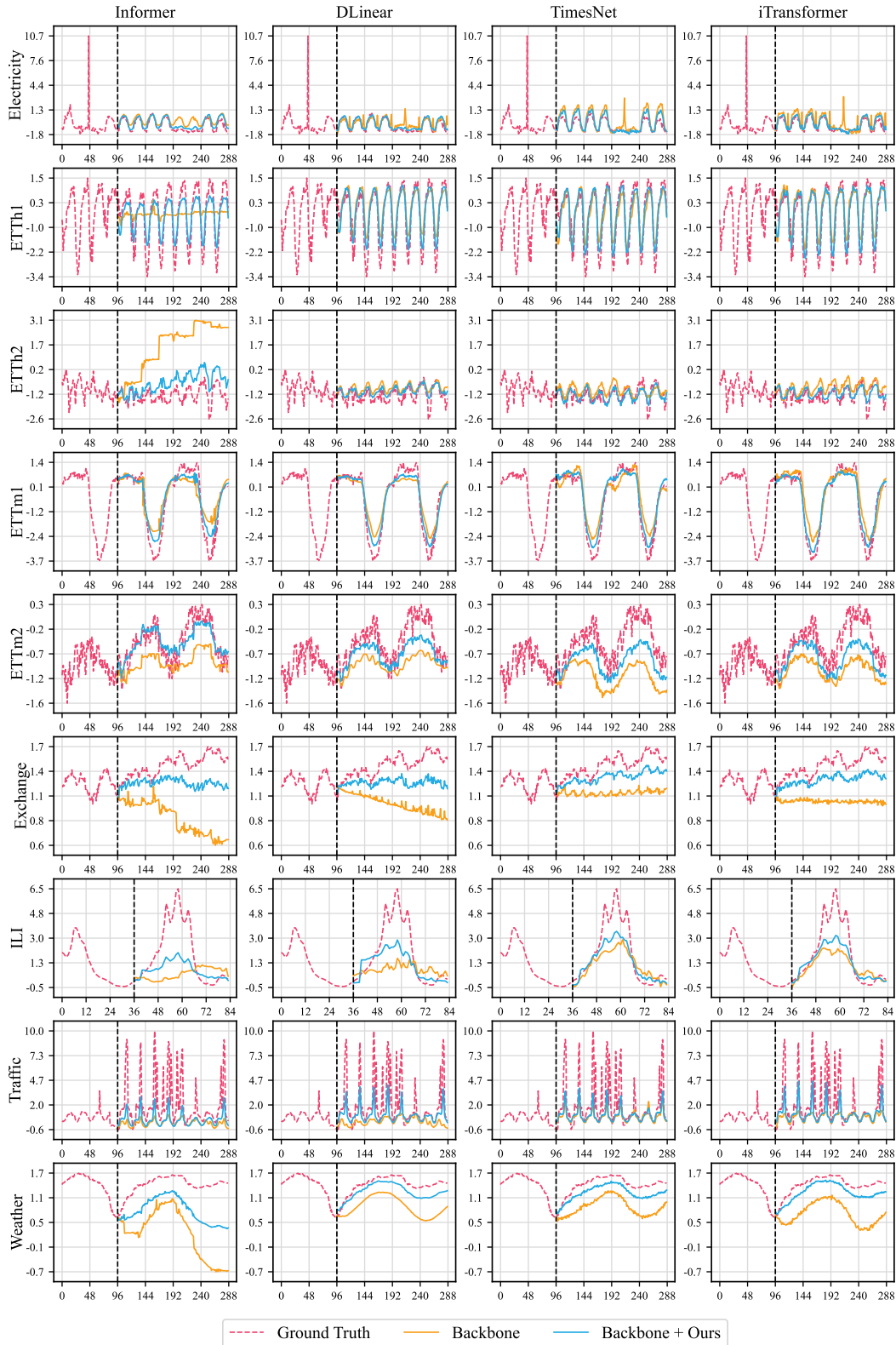


Figure 5: The complete illustration of prediction showcases among GLAFF and mainstream baselines.

corresponding licenses (Appendix A.1 and Appendix A.2). There is no potential ethical risk or negative social impact.

D Limitation

While GLAFF exhibits encouraging performance on benchmark datasets, it is subject to certain limitations. As a model-agnostic and plug-and-play framework, GLAFF incurs considerable computation costs attributed to the utilization of stacked attention blocks in Attention-based Mapper (Appendix B.4). Presently, with hardware resources evolving rapidly, this computation costs may not affect the training and deployment of GLAFF in most scenarios. However, GLAFF will likely encounter operational challenges in resource-constrained edge devices, thus restricting its applicability. In future work, we plan to explore lighter weight and more efficient architectures, such as dilated convolutional or graph neural networks, to replace the conventional attention mechanism.